Chemical Composition Effects on the Creep of Type 316 and 16-8-2 Stainless Steel Weld Metal

A combination of B, P and Ti appears to have a beneficial effect on strength and ductility

BY R. L. KLUEH AND D. P. EDMONDS

ABSTRACT. Alloying additions of titanium, boron, and phosphorus are known to affect the elevated-temperature strength and ductility of austenitic stainless steel weld metals. We studied the effect of these elements on the creep-rupture properties of type 316 stainless steel and 16-8-2 weld metals. Creep-rupture tests were made at 649°C (1200°F) on specimens taken from gas tungsten arc welds deposited with commercial and experimental filler wires. Additions of about 0.3, 0.4, and 0.8% Ti to the commercial composition for type 316 stainless steel increased its strength and ductility over those of welds made with a commercial filler wire. The maximum effect of titanium was apparent in the 0.4% Ti alloy, which had the best strength and ductility. Boron and phosphorus additions to the optimum titanium composition led to excellent long-term strength and ductility. The results for the type 16-8-2 weld metal under similar test conditions also demonstrated that additions of titanium, boron, and phosphorus led to significantly improved strength and ductility.

Introduction

We previously reported on creep-rupture studies designed to determine the effect of Si, B, P, and Ti additions to the base composition for type 308 stainless steel weld metal deposited by the gas tungsten arc process (Ref. 1). It was found that the addition of "controlled residual elements" (CRE) B, P, and Ti in concentrations of ~0.006% B, 0.041% P, and 0.5% Ti gives rise to increased strength and ductility. In this paper we will report on the effect of CRE additions to types 316 and 16-8-2 stainless steel weld metals.

This research was sponsored by Breeder Technology Projects, U. S. Department of Energy, under contract DE-AC05-840R21400 with Martin Marietta Energy Systems, Inc.

R. L. KLUEH is with the Metals and Ceramics Division, Oak Ridge National Laboratory, Oak Ridge, Tenn. D. P. EDMONDS is with Babcock and Wilcox Research and Development Division, Alliance, Ohio.

Experimental

Small experimental heats of types 316 and 16-8-2 stainless steel were melted, cast, and fabricated into 3.2 mm (⅛ in.) diameter filler wire. Selected additions of P, B, and Ti were made to these heats.

All the test welds were made in 13 mm (0.51 in.) thick stainless steel plates by use of a 75 deg included angle V-groove joint. Both type 316 and the 16-8-2 welds were made in type 316 plates. The welds were made by the manual GTAW process and stringer-bead techniques with average welding conditions of 190 A and 17 V, direct current electrode negative (DCEN). All welds used pure argon shielding gas.

All-weld-metal buttonhead specimens with a 3.2 mm (⅛ in.) diameter by 28.6 mm (1.1 in.) long gage section parallel to the welding direction were machined from each test weld. The center of each specimen coincided with the middle of the weld about 5 mm (0.2 in.) below the top surface of the weld. These specimens were tested at 649°C (1200°F) in air at stress levels intended to produce rupture times from 10 to 100 to several thousand hours. The load was applied gradually by mechanical and/or hydraulic devices. Extensometers mounted on the grips were used to monitor creep strains to within ±1%, with the total elongation and reduction of area being measured directly by fitting the fractured specimens together. Rupture data only are considered in this report.

Results

Type 316 Stainless Steel

The effect of titanium was determined from heats for which we attempted to obtain approximately 0.3, 0.5, and 1.0% Ti. For the latter two heats, less than the desired titanium concentration was obtained—Table 1. The measured titanium concentrations were 0.29, 0.36, and 0.83%.

Table 1—Chemical Composition of Experimental Type 316 Stainless Steel Filler Metal

Filler Metal[a]	Composition (wt-%) Cr	Ni	Mo	C	B	P	Ti	Si	Mn
Commercial	18.9	13.0	2.2	0.004	0.0004	0.023	<0.02	0.044	1.75
0.3% Ti	17.5	14.0	2.5	0.047	<0.005	0.005	0.29	0.03	1.41
0.5% Ti[b]	18.7	13.0	2.3	0.047	0.001	0.028	0.36	0.54	1.71
1.0% Ti[b]	18.1	13.1	2.2	0.055	0.001	0.021	0.83	0.58	1.72
0.006% B, 0.042% P	18.0	13.0	2.4	0.039	0.007	0.050	0.01	0.51	1.74
0.006% B, 0.042% P, 0.5% Ti[b]	18.6	13.0	2.3	0.047	0.006	0.046	0.37	0.54	1.73

[a]Nominal intended compositions.
[b]Actual composition was less than intended.

An increase in titanium from 0.29 to 0.36% led to a large increase in rupture strength—Fig. 1A. The rupture strength for the alloy with the most titanium (0.83%) fell below that for the 0.29% Ti alloy. Thus, a peak in strength occurs with titanium concentration. All three titanium alloys were stronger than the commercial alloy studied.

In addition to improving the strength, titanium also improved ductility—Fig. 1B. The alloy with the intermediate titanium concentration was both the strongest and the most ductile. The low-titanium alloy had the lowest ductility. All three titanium alloys had better ductility than the commercial alloy.

The alloy with approximately 0.006% B and 0.042% P was not weldable because of hot cracking. However, an alloy with approximately 0.37% Ti, 0.006% B, and 0.045% P was weldable. For the long-time creep tests, the welds from this alloy showed strength and ductility comparable to or better than that of the 0.36% Ti alloy—Fig. 1. Thus, as with type 308 stainless steel weld metal (Ref. 1), a combination of titanium, boron, and phosphorus in type 316 stainless steel also led to weld metal with superior strength and ductility (at long rupture times).

Visual observations on fractured specimens reflected the ductility measurements. The fractures on specimens from welds made with the commercial filler metal showed little or no necking; only the specimens subjected to short-time tests displayed necks. The results were similar for the welds with 0.29% Ti. The specimens with 0.37% Ti showed considerably more necking, and a decrease in neck formation occurred with decreasing stress. The welds with 0.83% Ti displayed decreasing amounts of necking with decreasing stress. Finally, the welds with 0.006% B, 0.045% P, and 0.37% Ti showed the formation of a ductile cup-cone type of fracture for all the tests.

The overall ferrite content for the type 316 stainless steel was less than that for the type 308 stainless steel (Ref. 1)—Table 2. Again, the titanium additions increased the ferrite number well above that for alloys without titanium, and the addition of boron and phosphorus to the 0.4% Ti alloy caused a decrease in ferrite number. During exposure at 649°C in a creep test, the ferrite number decreased to zero after about 500 h.

Because of the smaller amount of δ-ferrite present in these welds, the microstructures were somewhat different from those for the type 308 stainless steel welds (Ref. 1)—Fig. 2. The addition of titanium again appeared to lead to a finer substructure.

Metallographic examination of the fractured specimens indicated that the commercial alloy showed considerable intersubstructural crack formation all along the specimen gage section (Fig. 3), with no necking prior to failure. The specimens with 0.29% Ti showed a small amount of neck formation. However, a considerable number of cracks occurred along the specimen gage length. The specimens from the 0.36% Ti weld showed somewhat more necking. In this case, holes formed very near the fracture surface. The specimens from the weld with the highest titanium content had very flat fractures. Intersubstructural cracks again formed along the specimen gage length. Finally, the specimens from the weld that contained boron, phosphorus, and titanium fractured after considerable necking—a highly ductile cup-cone type of fracture. Only a few holes, which are indicative of a highly ductile fracture, formed near the fracture surface.

If we attempt to relate the fracture modes to the weld metal microstructures

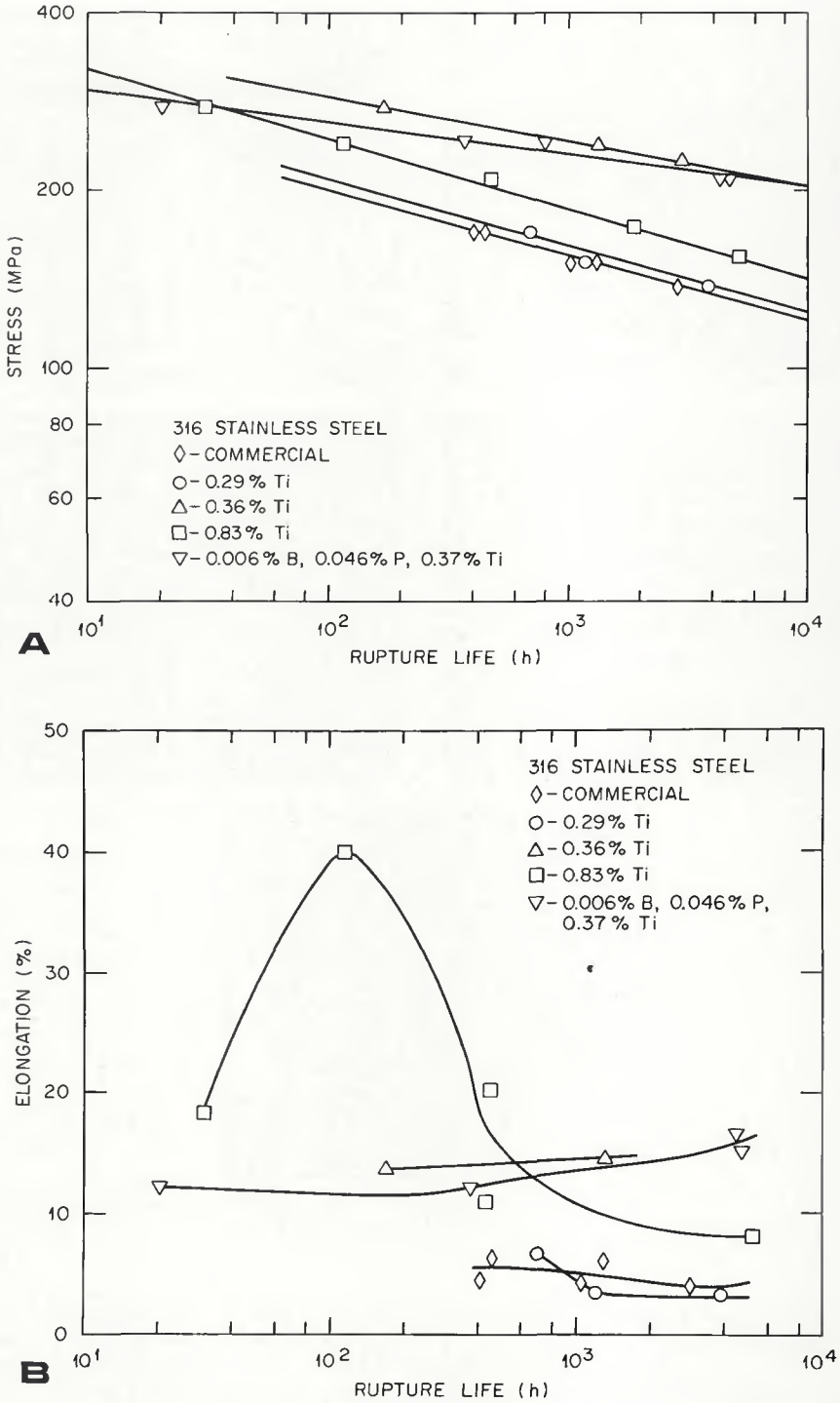

Fig. 1—Type 316 stainless steel welds deposited with commercial and experimental filler wires. A—Stress-rupture curves; B—Total elongation plotted against rupture life

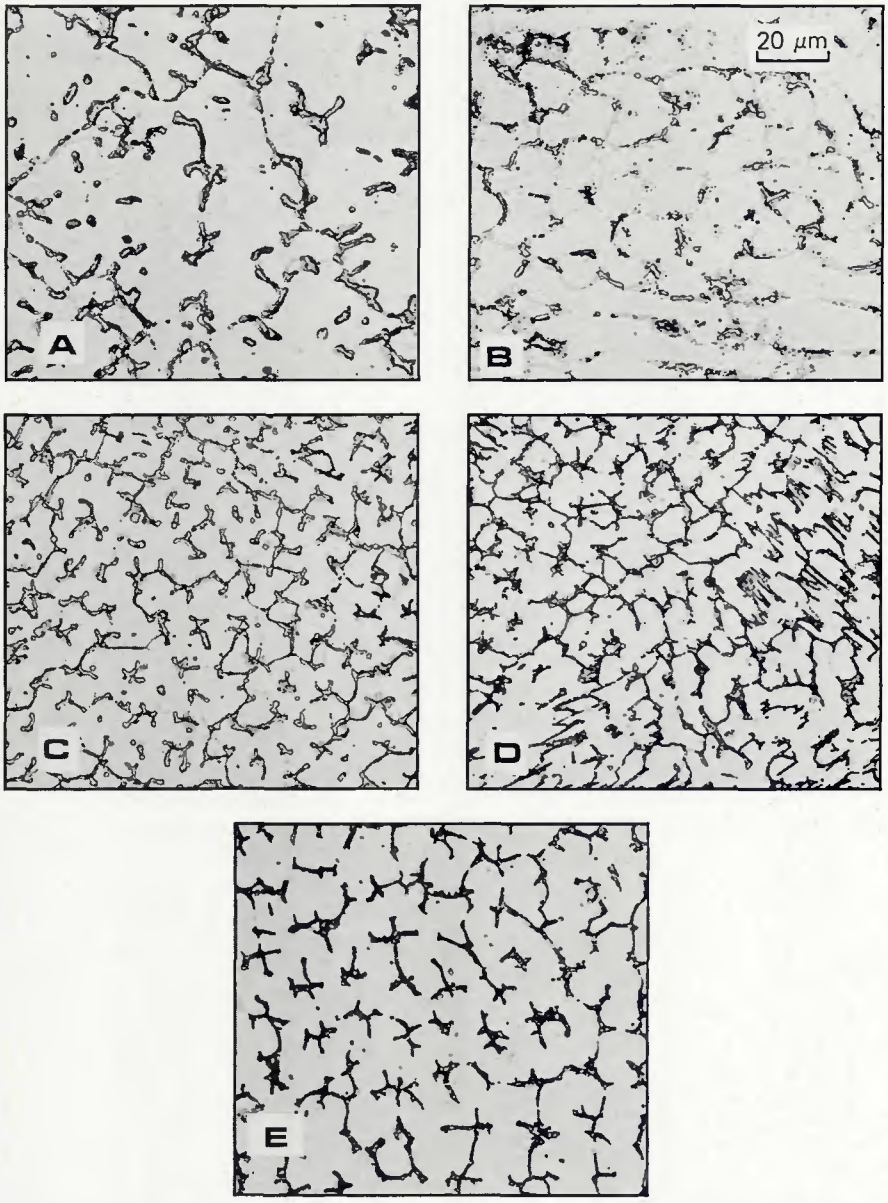

Fig. 2—Microstructure of gas tungsten arc type 316 stainless steel weld metal deposited with A—commercial filler wire and with experimental filler wires containing: B—0.29% Ti; C—0.36% Ti; D—0.83% Ti; and E—0.006% B, 0.045% P, and 0.37% Ti

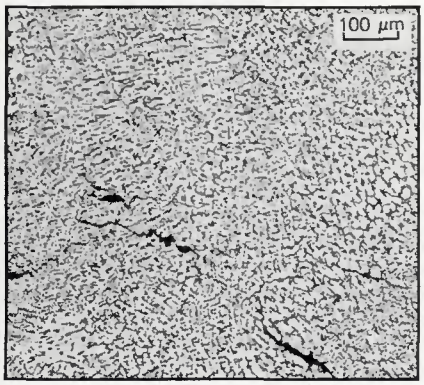

Fig. 3—Cracks in gage length of a gas tungsten arc type 316 stainless steel weld metal specimen from a weld deposited with a commercial filler wire

(Fig. 2), it appears that the welds with superior strength and ductility were those with an intermediate ferrite content (ferrite numbers of 5.5 to 6.5—Table 2). The specimens from welds with low ferrite content (ferrite numbers of 1 to 3.5) and high ferrite content (ferrite numbers of 8) were weaker and developed intersubstructural cracks. The welds with the intermediate ferrite content (Figs. 2C and 2E) had a relatively fine microstructure with the δ-ferrite much more interconnected than for the low-ferrite welds (Figs. 2A and 2B), but not as interconnected as it was for the high-ferrite 0.83% Ti alloy—Fig. 2D. In none of the alloys that contain titanium was there an indication of a precipitate in the light-etching austenite.

Table 2—Ferrite Number for Type 316 Stainless Steel Experimental Welds

Weld	Average Ferrite Number, As Welded[a]
Commercial (V-1)	2.8
Commercial (V-2)	3.1
0.006% B, 0.042% P (V-116)	2.0
0.006% B, 0.042% P (V-117)	1.7
0.29% Ti (V-44)	1.4
0.36% Ti (V-123)	5.5
0.36% (V-124)	6.1
0.83% Ti (V-126)	8.0[b]
0.83% Ti (V-128)	8.0[c]
0.0006% B, 0.046% P, 0.37% Ti (V-122)	6.4[d]
0.0006% B, 0.046% P, 0.37% Ti (V-129)	6.4

[a]After creep test at 649°C of >500 h, the ferrite number was essentially zero.
[b]Ferrite number varied from crown to root (range: 9.6–5.6).
[c]Ferrite number varied from crown to root (range: 9.0–5.2).
[d]Ferrite number varied from crown to root (range: 7.3–4.4).

16-8-2 Weld Metal

We attempted to prepare 16-8-2 filler metal alloys with 0.5 and 1.0% Ti, with 0.006% B and 0.042% P, and with 0.006% B, 0.042% P, and 0.5% Ti—Table 3. Again, the actual chemical compositions did not always meet the intended compositions (0.38% Ti instead of 0.5%; 0.79% Ti instead of 1.0%; ~0.003% B in the boron-phosphorus alloy instead of 0.006%; and 0.004% B, 0.036% P, and 0.39% Ti in the composition intended for 0.006% B, 0.042% P, and 0.5% Ti alloy).* The creep-rupture results showed considerably more scatter than observed in the types 308 (Ref. 1) and 316 stainless steel filler metals.

Figure 4 shows creep-rupture results for the experimental titanium heats and data from welds made with a commercial heat (we obtained data from welds made from nine different commercial heats of filler wire; the data shown are from the strongest of those heats). The data from different welds made from the same heat of wire for the 0.79% Ti alloy showed considerable variation, although the curves appear to converge at long rupture times. The stress-rupture curve for the 0.38% Ti weld lies above the 0.79% Ti

**Note in Table 3 that for the two 0.5% Ti and two 1.0% Ti heats listed, there is a difference in silicon content. The study on the type 308 stainless steel weld metal indicated there was no silicon effect. Not enough data were obtained in this study to determine if silicon affects the behavior of 16-8-2 weld metal.*

Table 3—Chemical Composition of Experimental Type 316 Stainless Steel Filler Metal

Weld	Filler Metal[a]	Composition (wt-%) Cr	Ni	Mo	C	B	P	Ti	Si	Mn
V-86	Commercial	15.16	8.43	1.28	0.07	0.001	0.019	0.01	0.42	1.44
V-115	Commercial	15.96	8.79	1.62	0.049		0.027		0.26	1.17
V-121	0.006% B, 0.042% P[b]	15.94	7.43	1.76	0.050	0.003	0.034	0.01	0.09	1.62
V-118	0.5% Ti[b]	15.50	7.20	1.75	0.054	0.001	0.018	0.39	0.09	1.60
V-125	0.5% Ti[b]	15.41	7.73	1.76	0.058	0.001	0.018	0.36	0.23	1.70
V-119	1.0% Ti[b]	15.15	7.28	1.75	0.060	0.001	0.019	0.78	0.009	1.57
V-127	1.0% Ti[b]	14.97	7.71	1.75	0.062	0.001	0.018	0.79	0.21	1.66
V-132	0.006% B, 0.042% P, 0.5% Ti[b]	15.24	7.67	1.76	0.058	0.004	0.036	0.39	0.013	1.70

[a]Nominal intended compositions.
[b]Actual composition was less than intended.

curve at high stresses and below it for low stresses. Thus, the addition of titanium gives a significantly stronger material than welds made with the commercial wire. If there is a strength peak with titanium concentration (as was true for types 308 and 316 stainless steel), it must be above 0.8% Ti.

In Fig. 5, the data for the heat with boron and phosphorus and with boron, phosphorus, and titanium are compared with one weld with about 0.38% Ti and the commercial heat. The strength of the heat with the boron and phosphorus additions was similar to that of the 0.38% Ti alloy. The creep-rupture strength for the weld that contained boron, phosphorus, and titanium was much greater than that for the other alloys.

The total elongation of the various welds showed relatively little difference for creep-rupture lifetimes between several hundred and several thousand hours—Fig. 6. The heat with a combination of boron, phosphorus, and titanium had excellent elongation for long rupture times.

Visual examination of fractured specimens indicated that the commercial alloys had quite ductile fractures with some neck formation. The amount of necking generally decreased with decreasing stress (increased rupture life). The considerably less ductile alloy with 0.38% Ti fractured with little neck formation. The high-titanium alloy displayed more ductility, although the fractures became flatter (less necking) with decreasing stress. The alloy with boron and phosphorus additions behaved like the high-titanium alloy, with the amount of necking decreasing (flatter fractures) with decreasing stress. Finally, the alloy to which boron, phosphorus, and titanium were added was extremely ductile, even the specimen that failed after 26,000 h, again indicating the beneficial effects of this combination of alloying additions.

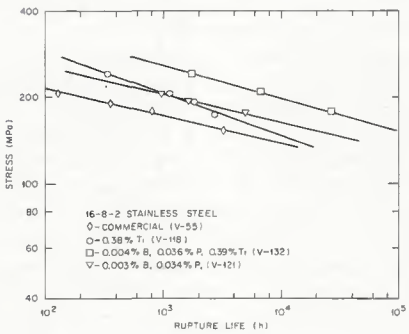

Fig. 5—Stress-rupture curves at 649°C for gas tungsten arc type 16-8-2 welds deposited with commercial and experimental filler wire

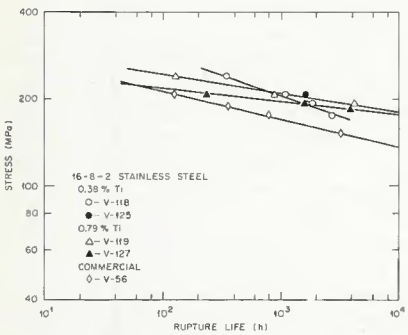

Fig. 4—Stress-rupture curves at 649°C for gas tungsten arc type 16-8-2 welds deposited with commercial and experimental filler wire

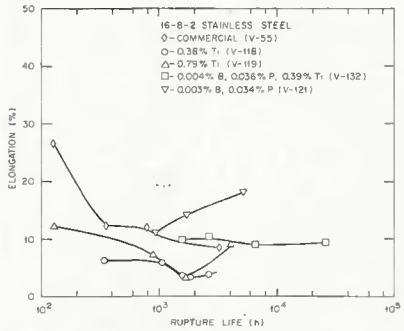

Fig. 6—Total elongation plotted against rupture life at 649°C for gas tungsten arc type 16-8-2 welds deposited with commercial and experimental filler wire

Ferrite content again reflected the effect of titanium: an increase in titanium increased the ferrite number—Table 4. The commercial alloys had the lowest ferrite numbers, the 0.79% Ti alloy the highest.

Metallographic observations on the specimens are in general agreement with the ductility measurements and the visual observations on the fractures. Reduced ductility coincided with an increase in the number of intersubstructural cracks in the specimen gage length, as was observed for the types 308 and 316 stainless steel weld metals.

Although microstructures differed from one weld to another, correlating these differences with the properties was difficult. Furthermore, every specimen had a range of microstructures on a given longitudinal section. The microstructures of the commercial alloys were quite coarse—Fig. 7A. Additions of titanium led to a much finer microstructure—Figs. 7B and 7C. The microstructure of the weld with boron and phosphorus additions was quite coarse—Fig. 7D. A still different structure was present for the alloy with titanium, boron, and phosphorus

Table 4—Ferrite Number for 16-8-2 Stainless Steel Experimental Welds

Weld	Average Ferrite Number, As Welded
Commercial (V-55)	3.2
Commercial (V-56)	2.9
0.003% B, 0.034% P (V-121)	4.0
0.38% Ti (V-118)	6.3
0.38% Ti (V-125)	4.9
0.79% Ti (V-119)	10.1[a]
0.79% Ti (V-127)	13.6[b]
0.004% B, 0.036% P, 0.4% Ti (V-132)	6.2

[a]Ferrite numbers varied greatly from crown to root (range: 18.0–4.2).
[b]Ferrite numbers varied greatly from crown to root (range: 18.3–5.1).

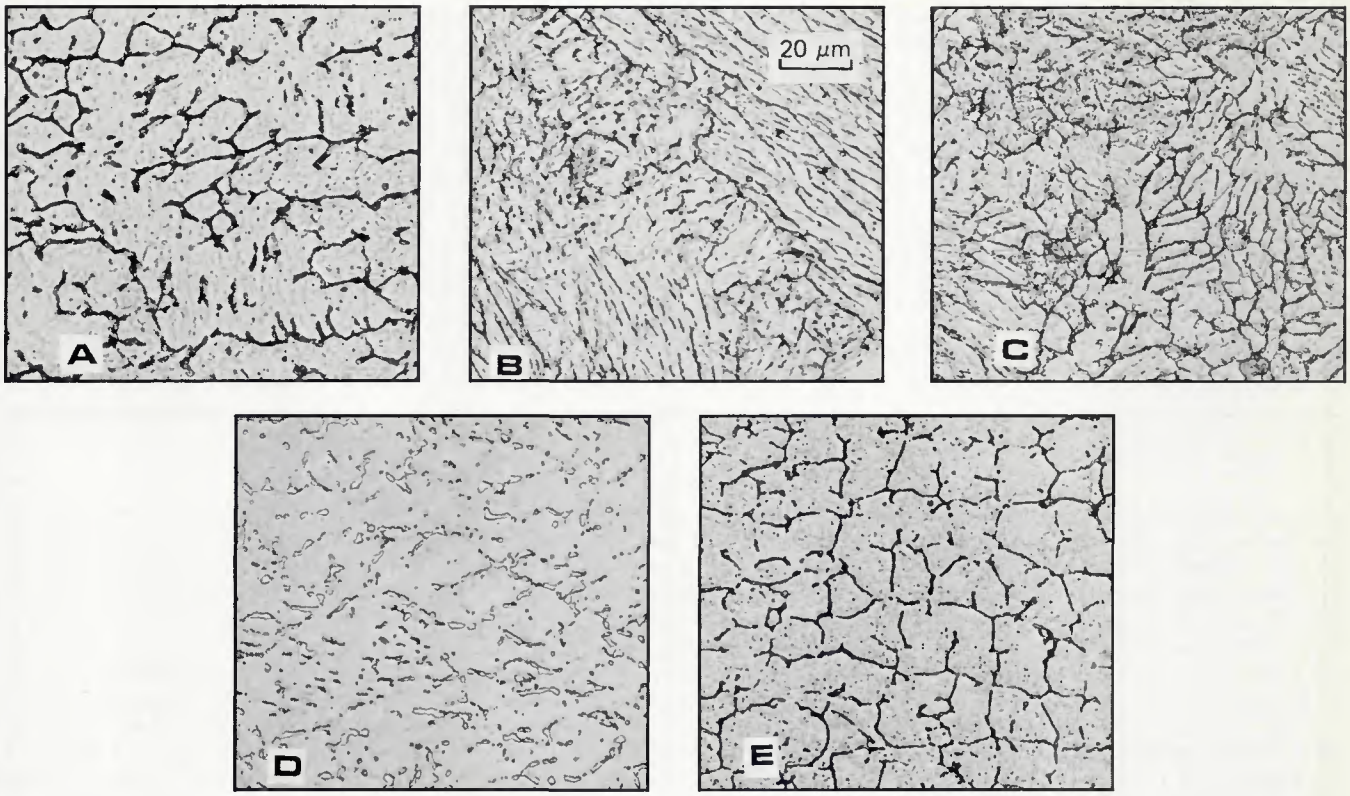

Fig. 7 — Microstructure of gas tungsten arc type 16-8-2 weld metal deposited with A — commercial filler wire and experimental wires containing: B — 0.38% Ti; C — 0.79% Ti; D — 0.003% B and 0.034% P; and E — 0.006% B, 0.042% P, and 0.38% Ti. Etchant: aqua regia

additions — Fig. 7E. However, we again emphasize that there was a range of microstructures for any given specimen, depending on the weld pass and the position in the pass relative to adjacent passes.

Discussion

The results of these studies, along with those previously reported (Ref. 1), demonstrated an effect of titanium, phosphorus, and boron on the strength and ductility of the GTA welds deposited with the austenitic stainless steel filler metals of types 308, 316, and 16-8-2. For all three materials, a combination of the three elements caused an increase in strength and ductility over the welds deposited with commercial filler metals and over those of the respective alloys with either titanium, phosphorus, or boron additions singularly or a combination of phosphorus and boron. In addition to the strength differences, the addition of titanium, phosphorus, and boron individually and in combination caused microstructural differences.

Several investigators have attempted to classify the microstructures of austenitic stainless steel welds on the basis of δ-ferrite morphologies (Refs. 2–5). There are basically two types of microstructures, termed "vermicular" (Refs. 2–5) and "lathy" (Ref. 4) or "acicular" (Ref. 5). These microstructures have been observed in the current studies — Fig. 8. The type of microstructure observed depended on the ferrite content: the vermicular structure occurred for a low volume fraction of ferrite (<6%) and was observed in type 316; the acicular occurred at higher ferrite contents (>12%) and was observed in type 308 (Ref. 1). Both types of structures were observed for the 16-8-2 weld metal.

As pointed out by David (Ref. 5), the ferrite content, as well as the microstructure, can vary across a given weld. These variations are the result of different cooling rates, weld metal composition differences due to base metal dilution, and dissolution of ferrite resulting from thermal cycles during subsequent weld passes. Such variations were noted in the welds made for this study. However, the microstructure generally showed little variation across the region in the center of the weld, where the 3.2 mm (⅛ in.) diameter test specimens were taken (the 16-8-2 welds showed the most variation in microstructure and the largest variation in ferrite number across the weld). The microstructures presented were repre-

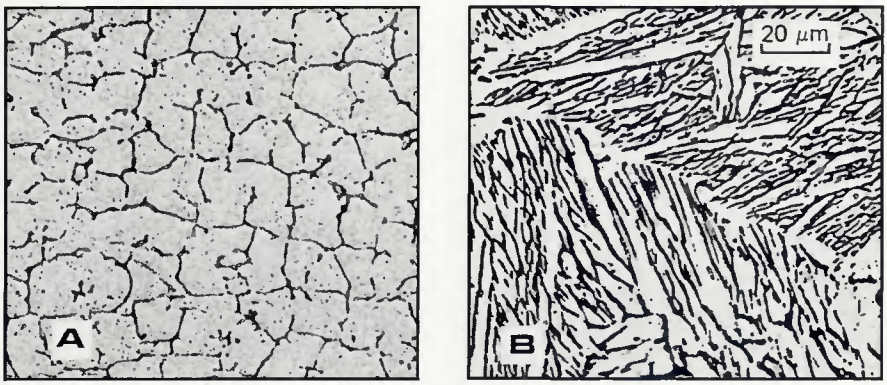

Fig. 8 — Examples of different types of weld metal microstructures observed: A — "Vermicular" structure of experimental type 16-8-2 weld with boron and phosphorus additions; B — "Lathy" or "acicular" structure of type 308 stainless steel weld with boron and phosphorus additions. Etchant: aqua regia

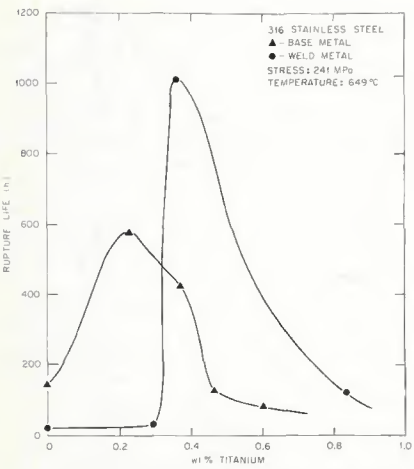

Fig. 9 — The rupture life plotted against titanium concentration for type 316 stainless steel weld metal and base metal. Source of base metal results: see Ref. 14

sentative of the position of the tensile specimens.

From an examination of the different microstructures of the types 308 stainless steel (Ref. 1) and 316 stainless steel weld metals, it appears that ferrite morphology must play a relatively minor role in the change in strength and ductility that accompanies the change in chemical composition. The type 308 stainless steel weld metals were basically acicular and the type 316 stainless steel basically vermicular, regardless of the composition. Both showed similar response to additions of titanium, boron, and phosphorus. Thus, the change in strength caused by these additions must be caused by something other than a microstructural change. In the case of the 16-8-2 weld metal, the large microstructural variability makes it much more difficult to make a statement concerning a relationship between ferrite morphology and composition, and an effect similar to the other two austenitic stainless steel weld metals is assumed.

In the type 308 stainless steel weld metal, we attributed the increased strength and ductility for the steel with boron, phosphorus, and titanium additions to changes in the precipitate morphology found when these elements were added to the commercial 308 stainless steel composition (Ref. 1). Titanium additions led to the formation of fine titanium-rich carbide, nitride, and sulphide precipitates that replace a relatively continuous grain boundary precipitate of $M_{23}C_6$ (Ref. 6). Boron and phosphorus can also lead to the breaking up of the continuous grain boundary precipitate and the formation of a finer $M_{23}C_6$ precipitate (Refs. 7–13). A similar effect of these elements is expected to occur in types 316 and 16-8-2 stainless steels.

Bloom, Leitnaker, and Stiegler studied the creep-rupture properties of titanium-modified type 316 stainless steel base metal and found that titanium had a similar effect to that found in the present studies for type 316 stainless steel weld metal. Creep tests were made at 241 MPa (35 ksi) and 650°C (1202°F) on type 316 stainless steel with 0, 0.23, 0.33, 0.46, and 0.60% Ti. In Fig. 9, these rupture-life data are compared with the data from the current study on type 316 stainless steel weld metal with 0, 0.29, 0.36, and 0.83% Ti. The similarity in behavior is obvious. Both the base metal and weld metal show peaks in rupture life at intermediate titanium concentrations. The peak for the weld metal is higher and appears to be displaced toward higher titanium concentrations.

The effect of the titanium in type 316 stainless steel base metal was attributed to fine titanium-rich precipitates in the austenite matrix (Ref. 14) (there is no δ-ferrite present in the base metal). In the weld metal, the δ-ferrite would be expected to be enriched in titanium, a ferrite-forming element. Thus, all the titanium added to the weld metal is not available for strengthening the austenite. This leads to displacement of the peak to higher concentrations. The titanium in the δ-ferrite and the formation of Ti(CN) and $Ti_2C_2S_4$ (Ref. 14) can probably account for the relatively small effect of titanium at low concentrations.

The difference in peak height may be due to the titanium concentrations for which measurements were made. That is, the peak strength of the base metal may occur for an alloy with titanium concentrations between 0.23 and 0.33%, or between 0 and 0.23% where no measurements were made. Another possibility is that the weld metal peak strength is enhanced by the δ-ferrite. However, the comparative strengths of weld metal and base metal on either side of the peaks do not support this latter hypothesis.

In addition to the change in precipitate morphology leading to improved ductility, Bloom, Leitnaker, and Stiegler (Ref. 14) also attributed the reduced tendency toward grain boundary cracking to the removal of surface-active elements such as sulfur and nitrogen. Titanium is known to remove these impurities from solution by forming $Ti_4C_2S_2$ and Ti(CN) (Ref. 15). Bloom and co-workers concluded that the removal of these elements from the grain boundaries could strengthen the boundaries and reduce grain boundary cracking (Ref. 14).

The analogous behavior of titanium in the weld metals and austenitic stainless steel base metals leads to the conclusion that the increased strength and ductility in the weld metal must be caused by processes similar to those that occur in the base metal. In addition to the beneficial role of titanium, phosphorus and boron also affected the creep-rupture properties as discussed above.

Summary and Conclusions

We investigated the effect of alloying additions on the elevated-temperature strength and ductility of austenitic stainless steel weld metals. Controlled additions of Si, Ti, P, and B were made to the commercial compositions for types 316 and 16-8-2 stainless steel filler metals. These experimental filler-metal alloys were then used to make GTA welds. Creep-rupture tests at 649°C (1200°F) were made on specimens taken from these welds.

A combination of approximately 0.042% P, 0.006% B, and 0.5% Ti in type 316 stainless steel gave an alloy with the best strength and ductility. However, as opposed to previous studies on type 308 stainless steel filler metal (Ref. 1), the strength superiority of this alloy over that with only the 0.5% Ti addition had to be inferred from extrapolations to low stresses (long rupture lifetimes). The improved ductility of the alloy with additions of B, P, and Ti was definitely established.

Creep-rupture studies on the 16-8-2 weld metals also established the beneficial effects of a combination of B, P, and Ti. The alloy with 0.04% B, 0.036% P, and 0.39% Ti had significantly better strength than any of the commercial or experimental heats tested. This improved strength was accompanied by an improved ductility for low-stress tests with long rupture times.

The effects of the titanium, phosphorus, and boron on the stress-rupture properties of the weld metal were compared with their effects in similar austenitic stainless steel base metal. Similar effects were observed, indicating that the processes that occur in the two types of microstructure are similar. This similarity occurred despite the fact that the weld metal microstructures contained large amounts of δ-ferrite that are not present in the base metals.

Acknowledgments

Special thanks are due to several people. E. Bolling carried out the experimental work. C. W. Houck did the metallography. The manuscript was reviewed by S. A. David and R. W. Swindeman. Frances Scarboro and Susan Hancher prepared the manuscript.

References

1. Klueh, R. L., and Edmonds, D. P. 1986. Chemical composition effects on the creep of type 308 stainless steel weld metal. *Welding*

Journal 65(1):1-s to 7-s.

2. Takalo, T., Suutala, N., and Moisio T. 1976. Influence of ferrite content on its morphology in some austenitic weld metals. *Metallurgical Transactions A* 7A:1591–1592.

3. Suutala, N., Takalo, T., and Moisio, T. 1979. The relationship between solidification and microstructure in austenitic and austenitic-ferritic stainless steel welds. *Metallurgical Transactions A* 7A:512–514.

4. Lai, J. K., *et al.* 1979. Variations in delta-ferrite content and morphology in a multipass type 316 weldment and their effect on creep rupture properties. *Welding and Fabrication in the Nuclear Industry,* pp. 233–238, British Nuclear Energy Society, London, England.

5. David, S. A. 1981. Ferrite morphology and variations in ferrite content in austenitic stainless steel welds. *Welding Journal* 60(4): 63-s to 71-s.

6. Vitek, J. M., and David, S. A. 1984. The solidification and aging behavior of types 308 and 308CRE stainless steel welds. *Welding Journal* 63(8):246-s to 253-s.

7. Allten, A. G., Chow, J. G. Y., and Simon, A. 1954. Precipitation hardening austenitic chromium-nickel steels containing high carbon and phosphorus. *Trans. Am. Soc. Met.* 45:948–972.

8. Froes, F. H., Wells, M. G. H., and Banerjee, B. R. 1968. Influence of phosphorus on the nucleation of $M_{23}C_6$ carbides in austenitic stainless steels. *Met. Sci. J.* 2:232–234.

9. Irvine, K. J., Llewellyn, D. T., and Pickering, F. B. 1961. High-strength austenitic stainless steels. *J. Iron Steel Inst.* 199:153–175.

10. Rowcliffe, A. F., and Nicholson, R. B. 1972. Quenching defects and precipitation in a phosphorus-containing austenitic stainless steel. *Acta Metallurgica* 20:143–155.

11. Henry, G., Plateau, J., Mercier, A., and Hochmann, J. 1963. Influence de faibles additions de bore sur la resistanceau fluage et la structure micrographique d'aciers derivant du type 18-10. *Rev. Metall.* 61:1221–1232.

12. Henry, G., *et al.* 1974. Orientation and morphology of $M_{23}(BC)_6$ precipitates in austenite grain boundaries. *Electron Microscopy 1974,* pp. 666–667, Australian Academy of Science, Canberra, A.C.T., Australia.

13. Thomas, B. J., and Henry, G. 1980. Boron in austenitic stainless steels. *Boron in Steels,* pp. 80–105, The Metallurgical Society of AIME, Warrendale, Pa.

14. Bloom, E. E., Leitnaker, J. M., and Stiegler, J. O. 1976. Effect of neutron irradiation on the microstructure and properties of titanium-stabilized type 316 stainless steels. *Nuclear Technology* 31:232–243.

15. Grot, A. S., and Spruiell, J. E. 1975. Microstructural stability of titanium-modified type 316 and type 321 stainless steel. *Metallurgical Transactions A* 6A:2023–2030.

Reminder to Authors

Please note that completed Author Application Forms and accompanying 500-word summaries must be mailed by July 15, 1986, to ensure consideration for the Professional Program of the 68th Annual AWS Convention, to be held March 22–27, 1987, in Chicago, Ill.

Call for Papers

Applications of Electron and Laser Beam Welding

Papers are being solicited for an AWS/AWI-sponsored international conference, "Applications of Electron and Laser Beam Welding," to be held in Hartford, Conn., September 16–17, 1987. The conference will cover present and potential production applications and laboratory innovations of both of these forms of energy beam technology. Specific topics will include heat treatment, thin material welding and cutting, dissimilar metal joining, and out-of-vacuum electron beam processing, among others. Application areas include shipbuilding, nuclear, transportation and consumer products. Conference proceedings will be published. Submit abstracts of 200–250 words by November 1986 to Dr. H. G. Ziegenfuss, Technical Director, American Welding Society, 550 N. W. LeJeune Rd., P. O. Box 351040, Miami, FL 33135. Full papers for those abstracts selected will be required by March 1, 1987.